

Na₂Ti₃O₇: Lowest Voltage Ever Reported Oxide Insertion Electrode for Sodium Ion Batteries

Premkumar Senguttuvan,^{†,‡,§} Gwenaëlle Rousse,[‡] Vincent Seznec,^{‡,§} Jean-Marie Tarascon,^{‡,§,#} and M.Rosa Palacín^{*,†,‡}


[†]Institut de Ciència de Materials de Barcelona (ICMAB-CSIC), Universitat Autònoma de Barcelona, E-08193 Bellaterra, Catalonia, Spain

[‡]ALISTORE ERI European Research Institute

[§]Laboratoire de Réactivité et Chimie des Solides, Université de Picardie Jules Verne, CNRS UMR6007, 33 rue Saint Leu 80039 Amiens, France

[‡]Institut de Minéralogie et de Physique des Milieux Condensés (IMPMC), UMR 7590 CNRS, Université Pierre et Marie Curie, Case courrier 115, 4 Place Jussieu, 75252 Paris Cedex 05, France

[#]Collège de France, 11 Place Marcelin Berthelot, 75005 Paris, France

 Supporting Information

KEYWORDS: sodium intercalation, sodium ion batteries, layered titanate, Na₂Ti₃O₇

Due to its success in the domain of power electronics, the lithium ion battery technology is currently being considered for electric vehicle propulsion and even electric grid storage.^{1,2} However, the implementation of a lithium based technology on a large scale faces controversial debates on lithium availability and cost. Alternative lower cost and sustainable chemistries would be specially suited for large scale applications even if they involve a penalty in energy density. The most appealing alternative is to use sodium, instead of lithium. Indeed, it exhibits a rich intercalation chemistry^{3,4} and its resources are in principle unlimited (high concentrations in seawater) being very easy to recuperate. Sodium technology has already been successfully implemented in today's commercialized high-temperature Na/S cells for MW storage and for Na/NiCl₂ ZEBRA-type systems for electric vehicles, both of which take advantage of the highly conducting solid beta-alumina ceramics at temperatures of ca. 300 °C. Mindful of these considerations, and within the current knowledge gained in Li-ion technology, a room temperature analogous Na-ion cell is a realistic target. If achieved, it would bring about a radical decrease in cost with respect to lithium ion technology while ensuring sustainability.

Electrochemical cells using sodium metal anodes and liquid electrolytes or solid polymer electrolytes were early on assembled using TiS₂, ternary transition metal oxides or even redox polymerization cathodes.^{5–7} Therefore, these systems were almost abandoned with the advent of the lithium ion technology. Recently, there has been a resurgence of interest with the assembly of a room temperature operation Na ion cell with liquid electrolyte using a carbonaceous negative electrode coupled to a sodium transition metal fluorophosphate positive electrode.⁸ Although a variety of phases with good features in terms of capacity and voltage that can potentially be used as positive electrodes have been identified, very few materials have been reported to be useful as negative electrodes (see Figure 1). Similarly to lithium ions, hard carbonaceous materials exhibit

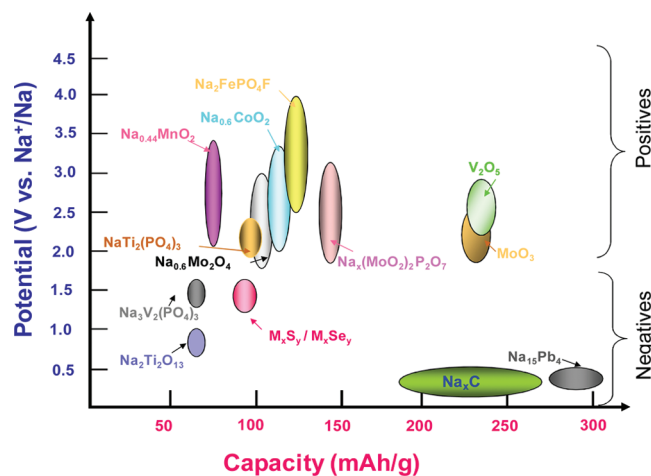


Figure 1. Potential versus capacity plot for materials having been reported to exhibit reversible sodium insertion and hence being potential electrode materials for sodium ion cells.

the ability to reversibly insert and deinsert sodium ions⁹ but exhibit higher capacity fading than their lithium counterparts.¹⁰

When it comes to transition metal oxides, the number of low potential lithium insertion compounds is rather limited owing to the competition of insertion vs conversion¹¹ reactions, the former being only favored for early 3d metal (Ti, V) oxides. Along that line, Na_xVO₂ was recently found to reversibly react with Na at ca. 1.5 V^{12,13} but sensibly lower operation voltages would be needed for enhanced energy density. While looking for alternative titanium-based systems we decided to investigate

Received: July 20, 2011

Revised: August 7, 2011

Published: August 30, 2011

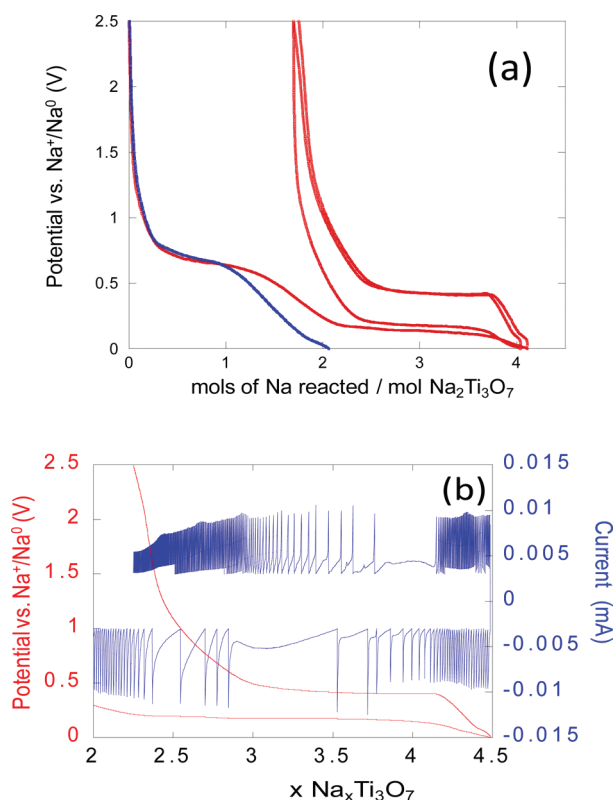


Figure 2. (a) Voltage versus composition profile for the electrochemical reduction of a blank electrode containing only carbon black (blue curve) and a composite electrode containing $\text{Na}_2\text{Ti}_3\text{O}_7$ and 30% carbon black (red curve) where the reversible insertion of ca. 2 mol of sodium ions per mol $\text{Na}_2\text{Ti}_3\text{O}_7$ is observed. (b) Stepwise potentiodynamic experiment (± 5 mV steps with a cut off intensity equivalent to $C/150$ galvanostatic rate).

$\text{Na}_2\text{Ti}_3\text{O}_7$. This phase has been known for long¹⁴ and studied for very diverse applications in sensors, catalysis, or toxic waste removal.^{15–19} Its structure consists of zigzag layers of titanium–oxygen octahedra with sodium ions in the interlayer space²⁰ that are easily exchanged.²¹ Its electrochemical behavior against lithium was tested between 1 and 3 V vs Li^+/Li^0 and shown to exhibit a gradually sloping profile between 1.6 and 1.0 V vs Li^+/Li^0 .²² Nonetheless, it had to the best of our knowledge never been tested in sodium-based cells. Pure $\text{Na}_2\text{Ti}_3\text{O}_7$ was prepared from anatase TiO_2 (>99.8%, Aldrich) and anhydrous Na_2CO_3 (>99.995%, Aldrich) mixtures with 10% excess of the latter with respect to stoichiometric amounts. These mixtures were milled and treated at 800 °C for 40 h with intermediate regrinding. Its X-ray diffraction (XRD, Cu $K\alpha$) pattern does not exhibit any impurity and is consistent with a well crystallized phase. A Rietveld refinement starting from the structural model of²³ was carried out including a bond valence sum analysis (BVS) using the Zachariasen formula: $V_i = \sum_j s_{ij} = \sum_j \exp\{(d_0 - d_{ij})/0.37\}$ and the parameters d_0 from.²⁴ Results are in full agreement with the expected structure and (IV) oxidation state for titanium. (Further details on the refinement together with typical scanning electron micrograph are given as Supporting Information.)

Preliminary electrochemical testing was carried out in two-electrode Swagelok cells using sodium (99.9% Aldrich) as a counter electrode in galvanostatic mode at a $C/25$ rate (i.e., 0.04 sodium/hour). The working electrode consisted of a powder mixture of

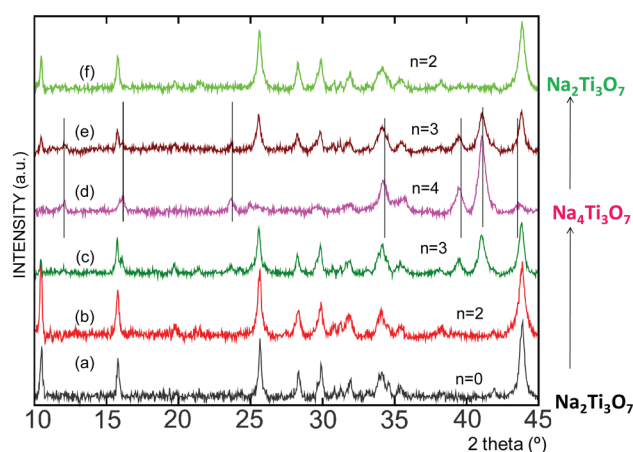


Figure 3. In situ X-ray diffraction study of a $\text{Na}_2\text{Ti}_3\text{O}_7/\text{Na}$ cell cycled between 2.5 and 0.01 V at a $C/50$ rate. For reasons of space, we have only reported the relevant XRD, the value of n corresponds to the mols of Na reacted per mol of $\text{Na}_2\text{Ti}_3\text{O}_7$ (see Figure 2a). The similarity of patterns a and b are in agreement with the sodium uptake at 0.7 V being related to carbon. Further reduction induces the appearance of a new set of peaks (marked with a line) corresponding to a new phase, which grows with increasing sodium uptake and is pure at the end of reduction.

the sample with 30% Super P carbon black and 1 M NaClO_4 in propylene carbonate (>99.7% Aldrich) was used as electrolyte. The voltage versus composition profile is shown in Figure 2a (red) together with the one achieved for an identical cell containing only carbon black (blue). The cell containing $\text{Na}_2\text{Ti}_3\text{O}_7$ exhibits an irreversible electrochemical process at ca. 0.7 V vs Na^+/Na^0 , which corresponds to reaction of carbon black used as additive, as deduced from comparison with the blank cell. (See corresponding derivative curves as Supporting Information). Further reduction takes place with the observation of a reversible plateau around 0.3 V vs Na^+/Na^0 with concomitant intercalation of ca. 2 additional sodium ions in the structure (i.e., reduction of 2/3 of Ti(IV) to Ti(III)). This process has been confirmed to be fully reversible (see the Supporting Information for capacity versus cycle number for the first 5 cycles). Stepwise potentiodynamic experiments using the EPS protocol of Thomson²⁵ (± 5 mV steps with a cut off intensity equivalent to a $C/150$ galvanostatic rate) (see Figure 2b) clearly indicate a two-phase redox process involving a phase transition.

The redox process was also followed by situ XRD (see Figure 3). No changes in the XRD pattern of the pristine $\text{Na}_2\text{Ti}_3\text{O}_7$ are observed during the first electrochemical process, in agreement of this being due to reaction for carbon black. In contrast, a biphasic process is observed during the plateau centered at 0.3 V vs Na^+/Na^0 during which the peaks of the pristine phase are found to progressively decrease while a new phase is found to appear, characterized by three intense peaks at 2θ values of 33.9, 39.2, and 40.7°. This phase is pure at the end of reduction (estimate composition $\text{Na}_4\text{Ti}_3\text{O}_7$). Upon reoxidation the process is reversed with increasing amounts of $\text{Na}_2\text{Ti}_3\text{O}_7$ appearing in the electrode. Once the oxidation process is finished, no traces of the $\text{Na}_4\text{Ti}_3\text{O}_7$ phase are observed in the XRD pattern.

Several attempts were carried out to model the structure of the fully reduced phase from the as obtained low resolution diffraction pattern. Indeed, since Na(1) and Na(2) 2e sites are completely filled in pristine $\text{Na}_2\text{Ti}_3\text{O}_7$, the insertion of additional sodium ions will probably force a structural rearrangement in

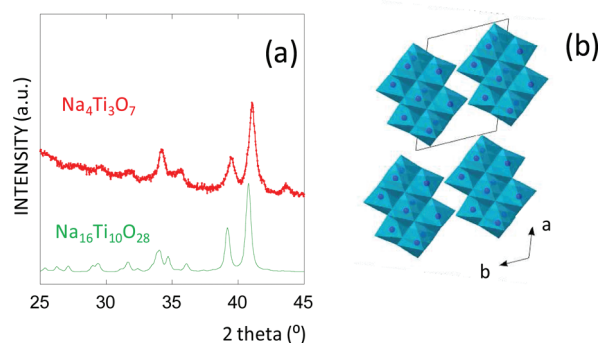


Figure 4. (a) Experimental XRD pattern for $\text{Na}_4\text{Ti}_3\text{O}_7$ (red dots) and simulated XRD pattern for $\text{Na}_{16}\text{Ti}_{10}\text{O}_{28}$ (green line) using the same profile parameters, where the analogy can be appreciated. (b) $\text{Na}_{16}\text{Ti}_{10}\text{O}_{28}$ crystal structure.

order to accommodate them. All attempts to reproduce the new set of peaks observed with a structure an $\text{Na}_2\text{Ti}_3\text{O}_7$ but with a larger interlayer space in order to place the two intercalated sodium ions failed. Interestingly, a sodium-rich compound of composition $\text{Na}_{16}\text{Ti}_{10}\text{O}_{28}$ ²⁶ exhibits three of its most intense reflections at the same 2θ values observed for $\text{Na}_4\text{Ti}_3\text{O}_7$ (see Figure 4a). Whether purely coincidentally or not, the stoichiometries of both phases are similar ($\text{Na}_4\text{Ti}_3\text{O}_7 = \text{Na}_{16}\text{Ti}_{12}\text{O}_{28}$) except for the titanium content and the mean titanium oxidation state ($\text{Na}_{16}\text{Ti}_{10}\text{O}_{28}$ contains Ti(IV)), which is in favor of a similar structural framework with all sodium ion available positions filled (else, further reduction to achieve 100% Ti(III) would take place). Both $\text{Na}_{16}\text{Ti}_{10}\text{O}_{28}$ and $\text{Na}_2\text{Ti}_3\text{O}_7$ have been reported to exist in the $\text{NaOH-TiO}_2\text{-H}_2\text{O}$ system, the former being favored for sodium rich compositions²⁷ and crystallizing in the P-1 space group, ($a = 10.51 \text{ \AA}$, $b = 8.34 \text{ \AA}$, $c = 8.51 \text{ \AA}$, $\alpha = 112.6^\circ$, $\beta = 104.1^\circ$, $\gamma = 102.2^\circ$). Its structure consists of clusters of ten TiO_6 octahedra with sodium atoms sitting in either an octahedral or a trigonal prismatic coordination between them. A general view of the structure is presented in Figure 4b. One might speculate that the structure of the inserted phase is pretty close to that adopted by $\text{Na}_{16}\text{Ti}_{10}\text{O}_{28}$, the clusters being most likely linked through the two supplementary titanium atoms. We are not yet able to propose a mechanism for this phase transition but further efforts are currently directed to collect synchrotron data for the fully reduced sample, which should throw new light on its nature and hopefully confirm our hypothesis.

In summary, we have found that $\text{Na}_2\text{Ti}_3\text{O}_7$ works as an effective low-voltage insertion sodium compound because of its ability to reversibly uptake 2 Na ions per formula unit (200 mAh/g) at an average potential of 0.3 V. To the best of our knowledge, this is the first ever reported oxide to reversibly react with sodium at such a low potential. Several improvements to the present work are immediately apparent and range from electrode optimization to the determination of the precise sodium insertion mechanism. Nevertheless, we believe that the result reported in this paper provides great opportunities in the development of room-temperature high-performing Na ion cells.²⁸

■ ASSOCIATED CONTENT

Supporting Information. Rietveld refinement for pristine $\text{Na}_2\text{Ti}_3\text{O}_7$ together with typical SEM micrograph. Derivative curves for plots depicted in Figure 2a and evolution of capacity

upon cycling. This material is available free of charge via the Internet at <http://pubs.acs.org/>.

■ AUTHOR INFORMATION

Corresponding Author

*E-mail: rosa.palacin@icmab.es.

■ ACKNOWLEDGMENT

We are grateful to the ALISTORE-ERI for support and helpful discussions and acknowledge Ministerio de Ciencia e Innovación (Spain) for grant MAT2011-24757.

■ REFERENCES

- (1) Armand, M.; Tarascon, J. M. *Nature* **2008**, *451*, 652.
- (2) Palacín, M. R. *Chem. Soc. Rev.* **2009**, *38*, 2565.
- (3) Whittingham, M. S. *Prog. Solid State Chem.* **1978**, *12*, 41.
- (4) Abraham, K. M. *Solid State Ionics* **1982**, *7*, 199.
- (5) Delmas, C.; Braconnier, J. J.; Fouassier, C.; Hagenmuller, P. *Solid State Ionics* **1981**, *3/4*, 165.
- (6) Ma, Y.; Doeff, M. M.; Visco, S. J.; Ma, Y.; Peng, M.; De Jonghe, L. C. *Electrochim. Acta* **1995**, *40*, 2205.
- (7) Doeff, M. M.; Visco, S. J.; De Jonghe, L. C. *J. Electrochem. Soc.* **1993**, *140*, 2726.
- (8) Barker, J.; Saidy, Y.; Swoyer, J. L. *Electrochem. Solid-State Lett.* **2003**, *6*, A1.
- (9) Stevens, D. A.; Dahn, J. R. *J. Electrochem. Soc.* **2000**, *147*, 1271.
- (10) Alcántara, R.; Jiménez Mateos, J. M.; Tirado, J. L. *J. Electrochem. Soc.* **2002**, *149*, A201.
- (11) Cabana, J.; Monconduit, L.; Larcher, D.; Palacín, M. R. *Adv. Mater.* **2010**, *22*, E170.
- (12) Didier, C.; Guignard, M.; Denage, C.; Szajwaj, O.; Ito, S.; Saasoune, I.; Darriet, J.; Delmas, C. *Electrochem. Solid-State Lett.* **2011**, *14*, A75.
- (13) Hamani, D.; Ati, M.; Tarascon, J. M.; Rozier, P. *Electrochem. Commun.* **2011**, doi:10.1016/j.elecom.2011.06.005
- (14) Naylor, B. F. *J. Am. Chem. Soc.* **1945**, *67*, 2120.
- (15) Holzinger, M.; Maier, J.; Sitte, W. *Solid State Ionics* **1996**, *86–8*, 1055.
- (16) Zhang, Y. Y.; Fu, W. Y.; Yang, H. B.; Li, M. H.; Li, Y. X.; Zhao, W. Y.; Sun, P.; Yuan, M. X.; Ma, D.; Liu, B. B.; Zhou, G. T. *Sens. Actuators, B* **2008**, *135*, 317.
- (17) Song, H. Y.; Liang, H. F.; Liu, T.; Liu, X. Q.; Meng, G. Y. *Mater. Res. Bull.* **2007**, *42*, 334.
- (18) Klerke, A.; Klitgaard, R.; Fehrmann, R. *Catal. Lett.* **2009**, *130*, 541.
- (19) Yang, D.; Zheng, Z.; Liu, H.; Zhu, H.; Ke, X.; Xu, Y.; Wu, D.; Sun, Y. *J. Phys. Chem. C* **2008**, *112*, 16275.
- (20) Andersson, S.; Wadsley, A. D. *Acta Crystallogr.* **1961**, *14*, 1245.
- (21) Izawa, H.; Kikkawa, S.; Koizumi, M. *J. Phys. Chem.* **1982**, *86*, 5023.
- (22) Chiba, K.; Kijima, N.; Takahashi, Y.; Idemoto, Y.; Akimoto, J. *Solid State Ionics* **2008**, *178*, 1725.
- (23) Yakubovich, O. V.; Kireev, V. V. *Crystallogr. Rep.* **2003**, *48*, 24.
- (24) Brown, I. D.; Altermatt, D. *Acta Crystallogr., Sect. B* **1985**, *41*, 244.
- (25) Thompson, A. H. *J. Electrochem. Soc.* **1979**, *126*, 608.
- (26) Mayer, M.; Perez, G. *Rev. Chim. Miner.* **1976**, *13*, 2.
- (27) Ilyushin, G. D. *Crystallogr. Reports* **2006**, *51*, 715.
- (28) Senguttuvan, P.; Palacín, M. R.; Tarascon, J. M. Patent Application FR11 56007, 2011.